EUROPEAN ORGANIZATION FOR NUCLEAR RESEARCH

L3 Note 2569
July 1, 2000

Preliminary Measurement of the $W^+W^-\gamma$ Cross Section and Direct Limits on Anomalous Quartic Gauge Boson Couplings at LEP

The L3 Collaboration

Abstract

The process $e^+e^- \to W^+W^-\gamma$ is analysed using the data collected with the L3 detector at LEP at a centre-of-mass energy of 188.6 GeV, corresponding to an integrated luminosity of $176.8\,pb^{-1}$. Based on a sample of 42 selected W^+W^- candidates containing an isolated hard photon, the $W^+W^-\gamma$ cross section, defined within phase-space cuts, is measured to be: $\sigma_{WW\gamma} = 290 \pm 80 \pm 16$ fb, consistent with the Standard Model expectation.

Including the process $e^+e^- \to \nu\bar{\nu}\gamma\gamma$ at centre-of-mass energies between 183 GeV and 202 GeV, limits are derived on anomalous contributions to the Standard Model quartic vertices $W^+W^-\gamma\gamma$ and $W^+W^-Z\gamma$ at 95% CL:

$$\begin{aligned} -0.035\ \text{GeV}^{-2} &< a_0/\Lambda^2 < 0.034\ \text{GeV}^{-2} \\ -0.07\ \text{GeV}^{-2} &< a_c/\Lambda^2 < 0.11\ \text{GeV}^{-2} \\ -0.41\ \text{GeV}^{-2} &< a_n/\Lambda^2 < 0.37\ \text{GeV}^{-2}. \end{aligned}$$

These results are preliminary.

Submitted to *2000 Summer Conferences*

Introduction

The LEP centre-of-mass energy for e^+e^- collisions is now well above the kinematic threshold for W-pair production allowing for the study of radiative W-pair production, $e^+e^- \to W^+W^-\gamma$. The Standard Model (SM) [1, 2] predicts the existence of quartic gauge couplings (QGCs), leading to $W^+W^-\gamma$ production via s-channel exchange of a γ or Z boson as shown in Figure 1a.

As the contribution of these two quartic Feynman diagrams with respect to the other competing diagrams, mainly initial-state radiation, is negligible at the LEP centre-of-mass energies, the process leading to the $W^+W^-\gamma$ final state could thus be sensitive to anomalous contributions to the SM quartic gauge-boson vertices $W^+W^-\gamma\gamma$ and $W^+W^-Z\gamma$.

The existence of Anomalous QGCs (AQGCs) would also affect the $e^+e^- \to \nu_e\bar{\nu}_e\gamma\gamma$ process via the W^+W^- fusion Feynman diagram containing the $W^+W^-\gamma\gamma$ vertex [3] (see Figure 1b). In the SM the reaction $e^+e^- \to \nu\bar{\nu}\gamma\gamma$ proceeds predominantly through s-channel Z exchange and t-channel W exchange, whereas the SM contribution from the W^+W^- fusion is negligible at LEP. AQGCs would enhance the $\nu\bar{\nu}\gamma\gamma$ production rate, especially for the hard tail of the photon energy distribution and for photons produced at large angles with respect to the beam direction.

Here we describe the cross section measurement for the process $e^+e^- \to W^+W^-\gamma$ and the determination of AQGCs using the data collected in 1998 with the L3 detector [4] at $\sqrt{s} = 188.6$ GeV (denoted as $\sqrt{s} = 189$ GeV hereafter) corresponding to an integrated luminosity of $176.8\,\mathrm{pb}^{-1}$. AQGCs are also independently determined using acoplanar photon-pair events with missing energy. This analysis is performed using the data at $\sqrt{s} = 189$ GeV, at $\sqrt{s} = 182.7$ GeV collected in 1997 (denoted as $\sqrt{s} = 183$ GeV hereafter) and at $\sqrt{s} = 192 - 202$ GeV collected in 1999 corresponding to a total integrated luminosity of $465\,\mathrm{pb}^{-1}$. The results derived on AQGCs from the $W^+W^-\gamma$ and $\nu\bar{\nu}\gamma\gamma$ channels are finally combined. These results are preliminary.

The search for anomalous contributions to the SM quartic couplings is performed within the theoretical framework of Reference [5, 6]. Recently, experimental measurements for these couplings have already been performed on final states with three vector bosons $W^+W^-\gamma$ [7] and $Z\gamma\gamma$ [8].

$W^+W^-\gamma$ Final State and Signal Definition

There are 14 Feynman diagrams at the tree level leading to the $W^+W^-\gamma$ final state, and many other diagrams corresponding to photons from the decay products of hadronic or leptonic W's. Only two of these, the quartic diagrams, are the processes in which we are interested. The other processes leading to the same final state are the initial state radiation (ISR), final state radiation (FSR), and radiation from the W boson itself.

The Monte Carlo used for the $W^+W^-\gamma$ cross section determination is KORALW [9]. This generator does not include the quartic coupling diagrams. Initial state multi-photon radiation is implemented in KORALW in the full photon phase space. FSR from charged leptons in the event up to double bremsstrahlung is included using the PHOTOS [10] package. Fragmentation processes of quarks into hadrons are made according to the JETSET [11] algorithm including photons in the parton shower. The background processes such as $e^+e^- \to Z/\gamma \to q\bar{q}(\gamma)$ and $e^+e^- \to ZZ \to 4f(\gamma)$ are simulated using PYTHIA [12]. For the $W^+W^-\gamma$ cross section measurement this modelling is sufficient since the contribution of all the other diagrams is very

small. The L3 detector response is simulated through the program GEANT [13].

In this analysis, the $W^+W^-\gamma$ signal is defined by the following phase-space cuts:

- $E_\gamma > 5$ GeV, where E_γ is the energy of the photon;
- $\theta_\gamma > 20^\circ$, where θ_γ is the angle between the photon and the beam axis,
- $\alpha_\gamma > 20^\circ$, where α_γ is the angle between the photon and the closest charged fermion.

These cuts are mainly chosen for experimental reasons, to optimise the photon identification, the background suppression, and for the detector acceptance of the tracking chamber. They also largely avoid any infrared and collinear singularities in the calculation of the signal cross section.

The predicted $W^+W^-\gamma$ cross section from KORALW corresponds to 272±4(stat) fb. In the EEWWG program [5], as suggested by the authors, the effect of undetected additional ISR collinear to the beam pipe is included [14] by implementing the EXCALIBUR [15] collinear radiator function in the code. The effect of the higher order radiative corrections is to move the effective centre-of-mass energy towards lower values, reducing the expected signal cross section by about 18%. The resulting EEWWG cross section corresponds to 233±12(theor) fb. This is used as the SM expectation in the anomalous coupling analysis, which leads to less stringent constraints on AQGCs. The theoretical uncertainty [14] is propagated to the AQGC determination. Consistent results are obtained with the YFSWW3 [16] MC which predicts 224±6(stat) fb.

Differences of this order in the predicted cross section with high transverse momentum photons are in general expected [17] between pure leading-log and leading-log plus matrix-element based calculations.

$W^+W^-\gamma$ Event Selection and Cross Section

The W-pair event selections used here are those reported in Reference [18]. Only the semileptonic and fully hadronic W-pair decay modes are considered. The number of selected data events and the expected number of signal and background events are shown in Table 1.

Decay Channel	Data	$\varepsilon_{\mathrm{WW}}$	N^{exp}_{TOT}	N^{exp}_{Bkgr}
$qqe\nu_e$	355	0.768±0.005	361	19
$qq\mu\nu_\mu$	364	0.834±0.002	375	19
$qq\tau\nu_\tau$	313	0.605±0.003	300	42
qqqq	1514	0.892±0.006	1486	296

Table 1: Number of observed events, selection efficiencies with statistical uncertainties, expected number of signal and background events for the various W^+W^- decay channels according to the SM prediction. The efficiencies shown here include the contribution of cross efficiencies from the other W-pair decay modes.

The photon selection in W^+W^- events is optimised for each four-fermion final state. Photons are selected by requiring energy deposition in the electromagnetic calorimeter not associated

with any track in the central detector, and low hadronic activity in a cone of half-opening angle of 7° around the electromagnetic cluster. The profile of the shower must be consistent with that of an electromagnetic particle. In addition, the highest energetic photon has to satisfy the same requirements of the signal definition (i.e., $E_\gamma > 5$ GeV, $\theta_\gamma > 20°$, and $\alpha_\gamma > 20°$ for the measured quantities). Figure 2 shows the distributions of E_γ, θ_γ, and α_γ, where for the last variable the direction of the reconstructed hadronic jet is assumed as the direction of the quark in the final state. In general, good agreement between the data and the SM expectation is observed.

Table 2 summarises the results for the applied selection criteria. In total 42 $W^+W^-\gamma$ events are selected, where 37.8±0.6 is the Monte Carlo expectation. The efficiency $\varepsilon_{WW\gamma}$ is defined as the number of selected KORALW events (regardless of any phase-space cuts) divided by the number of generated MC events satisfying the signal definition. It accounts for small possible migration effects of events from outside the signal region into the selected sample due to the finite detector resolution.

Decay Channel	Data	$\varepsilon_{WW\gamma}$	N^{exp}_{TOT}	$N^{exp}_{FSR} + N^{exp}_{Bkgr}$
$qqe\nu_e\gamma$	6	0.483±0.025	5.85±0.26	2.26±0.14
$qq\mu\nu_\mu\gamma$	5	0.547±0.027	6.87±0.28	2.88±0.17
$qq\tau\nu_\tau\gamma$	7	0.351±0.018	4.63±0.22	2.05±0.14
$qqqq\gamma$	24	0.504±0.016	20.4±0.38	9.23±0.26
Total	42	–	37.8±0.6	16.4±0.4

Table 2: Number of observed events, selection efficiencies with statistical uncertainties and expected number of total and background events including final state radiation.

The $W^+W^-\gamma$ cross section is evaluated channel by channel and then combined enforcing W-pair branching fractions. The result is:

$$\sigma_{WW\gamma} \;=\; 290 \pm 80 \pm 16 \text{ fb}\,,$$

where the first error is statistical and the second systematic. The measurement is in good agreement with both the KORALW and EEWWG SM expectations.

Figure 3 shows the obtained result together with the total $W^+W^-\gamma$ predicted cross section from the EEWWG Monte Carlo as a function of the centre-of-mass energy.

The systematic uncertainties arising in the inclusive W-pair event selections [18] are propagated to the final measurement and correspond to an uncertainty of ±6.3 fb. Other possible systematic biases due to detector effects such as electro-magnetic cluster resolution, angular resolution, and calorimetric energy scale uncertainty are found to have negligible effect on the final result.

The total systematic uncertainty is dominated by the JETSET modelling of photons from meson decays (π^0, η). To estimate this effect, a data sample of 3.9 pb^{-1} collected in 1998 at the Z pole ($\sqrt{s} = 91$ GeV) is studied. The same photon identification criteria are applied to the selected $Z \to q\bar{q}$ events. An overall excess of about (20±10)% in the photon rate is found in data with respect to the PYTHIA Monte Carlo which implements the same JETSET fragmentation algorithm and particle decays used in KORALW. A correction factor given by the ratio of photon production rates in data and MC is determined as a function of the photon energy.

This correction is applied to the background component of $q\bar{q}\gamma$ MC events as well as to the hadronic side of the $W^+W^-\gamma$ MC events. The uncertainty on this correction is propagated to the measurement as a systematic uncertainty on the $W^+W^-\gamma$ cross section which corresponds to ± 15 fb. The total systematic error on the cross section determination is small compared to the statistical error.

Determination of Anomalous Quartic Gauge Couplings

The selected $W^+W^-\gamma$ events allow us to constrain anomalous contributions to the SM quartic gauge boson vertices. In the framework of Reference [5, 6], the extended Lagrangian includes new dimension-6 operators,

$$\begin{aligned}
\mathcal{L}_0 &= -\frac{e^2}{16}\frac{a_0}{\Lambda^2} F^{\mu\nu} F_{\mu\nu} \overrightarrow{W^\alpha} \cdot \overrightarrow{W_\alpha} \\
\mathcal{L}_c &= -\frac{e^2}{16}\frac{a_c}{\Lambda^2} F^{\mu\alpha} F_{\mu\beta} \overrightarrow{W^\beta} \cdot \overrightarrow{W_\alpha} \\
\mathcal{L}_n &= -\frac{ie^2}{16}\frac{a_n}{\Lambda^2} \epsilon_{ijk} W^{(i)}_{\mu\alpha} W^{(j)}_{\nu} W^{(k)\alpha} F^{\mu\nu},
\end{aligned}$$

where a_0/Λ^2, a_c/Λ^2, and a_n/Λ^2 are the AQGCs, and Λ represents the energy scale for new physics. The two parameters a_0/Λ^2 and a_c/Λ^2, which are separately C and P conserving, generate anomalous $W^+W^-\gamma\gamma$ and $ZZ\gamma\gamma$ vertices. The term a_n/Λ^2, which is CP violating, gives rise to an anomalous contribution to $W^+W^-Z\gamma$. Although there are already direct [7, 8] and indirect [19] limits on a_0/Λ^2 and a_c/Λ^2 , only the study of $W^+W^-\gamma$ events allows for a direct measurement of the anomalous coupling a_n/Λ^2 through the $W^+W^-Z\gamma$ vertex.

The EEWWG program implements the effects of the Anomalous QGCs through the extended SM Lagrangian. Figure 3 shows how the anomalous coupling a_n/Λ^2 manifests itself through a deviation of the total cross section.

The anomalous component from the above operators is linear in the photon energy at the matrix element level [5]. This implies that also the shape of the photon spectrum is affected by AQGCs, in particular, for the hard part of the energy distribution. The expected distribution for any value of any of the three AQGCs is obtained by reweighting each KORALW MC event with the ratio $\mathcal{W}(E_\gamma; a_0, a_c, a_n)$ of the known differential distributions of E_γ at generator level:

$$\mathcal{W}(E_\gamma, a_0, a_c, a_n) = \frac{d\sigma^{EEWWG}}{dE_\gamma}(a_0, a_c, a_n) \Big/ \frac{d\sigma^{KORALW}}{dE_\gamma} .$$

The reweighting procedure is applied only to the ISR component of the MC selected sample, while the FSR (from KORALW) and the background components of accepted events are kept fixed. The possible dependence of the selection efficiency on the photon polar angle and on the angular separation from the charged fermions in the event is found to be negligible.

Both the shape and the normalisation of the observed photon spectrum in the range from 5 GeV to 30 GeV are used in a maximum-likelihood fit to each of the anomalous couplings a_0/Λ^2, a_c/Λ^2 and a_n/Λ^2, fixing the other two to zero. The effects of the same systematic uncertainties described for the cross section measurement are included, yielding:

$$\begin{aligned}
a_0/\Lambda^2 &= 0.012^{+0.019}_{-0.034} \pm 0.008 \text{ GeV}^{-2} \\
a_c/\Lambda^2 &= 0.06^{+0.04}_{-0.09} \pm 0.02 \text{ GeV}^{-2} \\
a_n/\Lambda^2 &= 0.08^{+0.17}_{-0.29} \pm 0.07 \text{ GeV}^{-2} ,
\end{aligned}$$

where the first error is statistical and the second systematic.

The 1-parameter limits at 95% CL are:

$$\begin{aligned} -0.045\ \text{GeV}^{-2} &< a_0/\Lambda^2 < 0.045\ \text{GeV}^{-2} \\ -0.08\ \text{GeV}^{-2} &< a_c/\Lambda^2 < 0.13\ \text{GeV}^{-2} \\ -0.41\ \text{GeV}^{-2} &< a_n/\Lambda^2 < 0.37\ \text{GeV}^{-2}. \end{aligned}$$

The results are in good agreement with the SM value of zero for each of the anomalous quartic gauge couplings.

The $e^+e^- \to \nu\bar{\nu}\gamma\gamma$ Process

The selection of acoplanar multi-photon events is identical to that described in Reference [20]. At least two photons with energies larger than 5 GeV and 1 GeV are required, with polar angles between 14° and 166°. The KORALZ [21] and NUNUGPV [22] Monte Carlo generators are used to model the $e^+e^- \to \nu\bar{\nu}\gamma\gamma$ process according to the SM. The effects of the AQGCs a_0/Λ^2 and a_c/Λ^2 are simulated using the EENUNUGGANO program [3]. Note that $\nu\bar{\nu}\gamma\gamma$ production is not sensitive to the a_n/Λ^2 coupling.

We select 14 events at $\sqrt{s} = 183$ GeV, 21 events at $\sqrt{s} = 189$ GeV and 49 events at $\sqrt{s} = 192 - 202$ GeV compared to a SM expectation of 13.3, 36.2 and 40.5 events respectively. Figures 4a and 4b show the two-photon recoil mass distributions at $\sqrt{s} = 189$ GeV and $\sqrt{s} = 192 - 202$ GeV, the predicted AQGC signals for a non-zero anomalous coupling a_0/Λ^2 are also shown. For a large fraction of the AQGCs signal the two-photon recoil mass M_{rec} is less than the mass of the Z, while almost no SM contribution is expected in this region. The cross section of the AQGC $\nu\bar{\nu}\gamma\gamma$ signal in the region $M_{rec} < M_{\mathrm{Z}}$ is shown in Figures 5a and 5b as a function of the anomalous coupling a_0/Λ^2 and of the centre-of-mass energy respectively.

The EENUNUGGANO program does not describe the effects of the SM s-channel Z exchange diagrams and the interference between these diagrams and the W^+W^- fusion diagram containing the $W^+W^-\gamma\gamma$ vertex. Therefore additional cuts are applied to suppress the SM contribution. The energy of both photons must be larger than 10 GeV. If both photons are in the barrel region ($|\cos\theta| < 0.7$), either the recoil mass must be less than 80 GeV or the sum of the photon energies must be larger than 100 GeV. If one or two photons are in the endcaps, where the SM contribution is larger, the recoil mass must be less than 75 GeV.

After applying these cuts no data event is selected, consistent with the SM expectation of about 0.15 events. The expected number of events for any AQGC value is calculated based on a sample of ten thousand simulated EENUNUGGANO events generated for several values of a_0/Λ^2 and a_c/Λ^2. Its matrix element is used to reweight the events to any AQGC value required, testing the procedure by comparing the reweighted distributions to distributions from samples generated at various values of AQGCs. In all cases good agreement is observed.

Since the EENUNUGGANO program does not include higher order corrections due to ISR, these effects are estimated by implementing the EXCALIBUR [15] collinear radiator function. The cross section is reduced by about 16% which is used in the following. The remaining theoretical uncertainty of 5% [14] is taken into account in the AQGC limits. The systematic uncertainty on the selection efficiency [20] gives a much smaller contribution.

The 95% CL upper limit on the number of expected events from the AQGC signal is obtained taking into account the systematic error on the accepted cross section; this corresponds to the

following 1-parameter limits at 95% CL:

$$\begin{aligned} -0.041 \text{ GeV}^{-2} &< a_0/\Lambda^2 < 0.040 \text{ GeV}^{-2} \\ -0.12 \text{ GeV}^{-2} &< a_c/\Lambda^2 < 0.12 \text{ GeV}^{-2}\,. \end{aligned}$$

Conclusion

Combining the results on a_0/Λ^2 and a_c/Λ^2 obtained from our analyses of $\mathrm{W^+W^-}\gamma$ and $\nu\bar{\nu}\gamma\gamma$ production, we obtain the following 1-parameter limits:

$$\begin{aligned} -0.035 \text{ GeV}^{-2} &< a_0/\Lambda^2 < 0.034 \text{ GeV}^{-2} \\ -0.07 \text{ GeV}^{-2} &< a_c/\Lambda^2 < 0.11 \text{ GeV}^{-2} \\ -0.41 \text{ GeV}^{-2} &< a_n/\Lambda^2 < 0.37 \text{ GeV}^{-2} \end{aligned}$$

at 95% CL. These results are in a good agreement with the SM expectations of zero for each anomalous quartic gauge boson coupling.

Acknowledgements

We thank J. W. Stirling and A. Werthenbach for providing us with the $\mathrm{e^+e^-} \to \mathrm{W^+W^-}\gamma$ and the $\mathrm{e^+e^-} \to \nu\bar{\nu}\gamma\gamma$ analytical calculations including AQGCs. We wish to express our gratitude to the CERN accelerator divisions for the superb performance and the continuous and successful upgrade of the LEP machine. We acknowledge the contributions of the engineers and technicians who have participated in the construction and maintenance of this experiment.

References

[1] S.L. Glashow, Nucl. Phys. **22** (1961) 579; A. Salam, in Elementary Particle Theory, ed. N. Svartholm, (Almqvist and Wiksell, Stockholm, 1968), p. 367; S. Weinberg, Phys. Rev. Lett. **19** (1967) 1264.

[2] M. Veltman, Nucl. Phys. **B7** (1968) 637; G.M.'t Hooft, Nucl. Phys. **B35** (1971) 167; G.M.'t Hooft and M. Veltman, Nucl. Phys. **B44** (1972) 189; Nucl. Phys. **B50** (1972) 318.

[3] J.W. Stirling and A. Werthenbach, Phys. Lett. **B466** (1999) 369.

[4] L3 Collab., B. Adeva *et al.*, Nucl. Instr. Meth. **A289** (1990) 35; J. A. Bakken *et al.*, Nucl. Instr. Meth. **A275** (1989) 81; O. Adriani *et al.*, Nucl. Instr. Meth. **A302** (1991) 53; B. Adeva *et al.*, Nucl. Instr. Meth. **A323** (1992) 109; K. Deiters *et al.*, Nucl. Instr. Meth. **A323** (1992) 162; M. Chemarin *et al.*, Nucl. Instr. Meth. **A349** (1994) 345; M. Acciarri *et al.*, Nucl. Instr. Meth. **A351** (1994) 300; G. Basti *et al.*, Nucl. Instr. Meth. **A374** (1996) 293; A. Adam *et al.*, Nucl. Instr. Meth. **A383** (1996) 342.

[5] J.W. Stirling and A. Werthenbach, Eur. Phys. J. **C14** (2000) 103.

[6] G. Belanger and F. Boudjema, Nucl. Phys. **B 288** (1992) 201.

[7] Opal Collab., G. Abbiendi *et al.*, Phys. Lett. **B471** (1999) 293.

[8] L3 Collab., M. Acciarri *et al.*, Phys. Lett. **B478** (2000) 34.

[9] KORALW V1.42, M. Skrzypek *et al.* Comp. Phys. Comm. **94** (1996) 216; Phys. Lett. **B372** (1996) 289.

[10] E. Barberio, B. van Eijk and Z. Was, Comp. Phys. Comm. **79** (1994) 291.

[11] T. Sjöstrand and H. U. Bengtsson, Comp. Phys. Comm. **46** (1987) 43.

[12] T. Sjöstrand, Comp. Phys. Comm. **82** (1994) 74.

[13] The L3 detector simulation is based on GEANT Version 3.15.
See R. Brun *et al.*, "GEANT 3", CERN DD/EE/84-1 (Revised), September 1987.
The GHEISHA program (H. Fesefeldt, RWTH Aachen Report PITHA 85/02 (1985)) is used to simulate hadronic interactions..

[14] J.W. Stirling and A. Werthenbach, private communication.

[15] F.A. Berends, R. Pittau and R. Kleiss Comp. Phys. Comm. **85** (1995) 437.

[16] S. Jadach, *et al.*, preprint UTHEP-00-0101, to appear.

[17] S. Jadach, private communication.

[18] L3 Collab., Preliminary Results on the Measurement of W-Pair Cross Sections in e^+e^- Interactions at $\sqrt{s} = 189$ GeV and W-Decay Branching Fractions, L3 Note 2376; submitted to the International Europhysics Conference High Energy Physics 99, Tampere, Finland, 15-21 July 1999.

[19] O.J.P. Eboli and M.C. Gonzales–Garcia, Phys. Lett. **B411** (1994) 381.

[20] L3 Collab., M. Acciarri *et al.*, Phys. Lett. **B444** (1998) 503, **B470** (1999) 268.

[21] The KORALZ version 4.03 is used.
S. Jadach, B.F.L. Ward and Z. Was, Comp. Phys. Comm. **79** (1994) 503.

[22] G. Montagna, *et al.*, Nucl. Phys. **B541** (1999) 31.

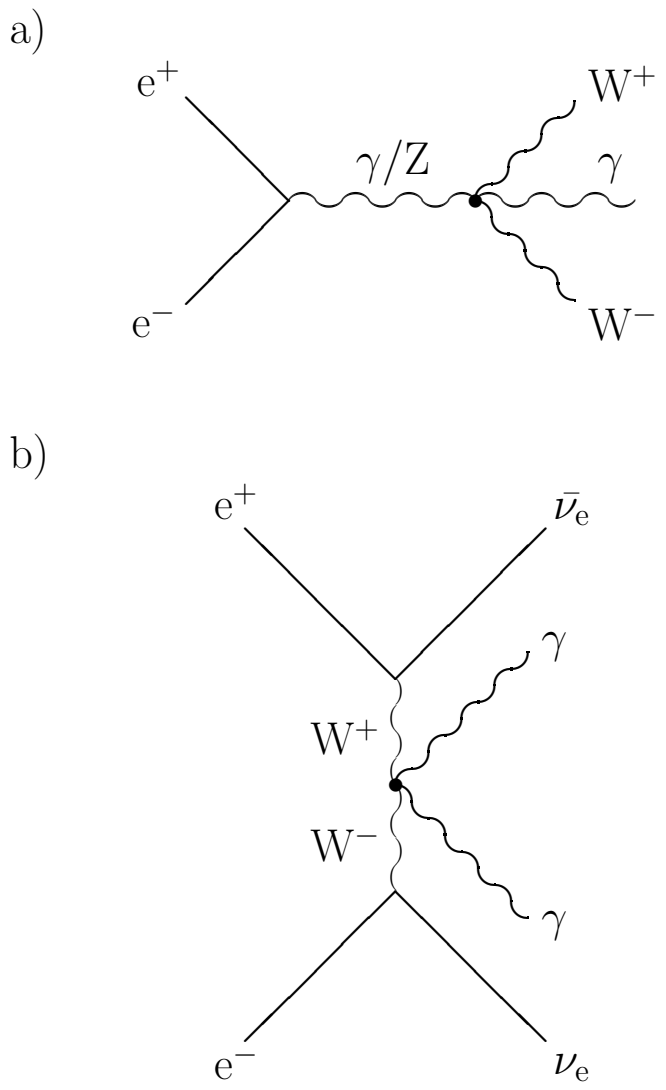

Figure 1: Feynman diagrams containing a four-boson vertex leading to the (a) $W^+W^-\gamma$ and (b) $\nu_e\bar{\nu}_e\gamma\gamma$ final states.

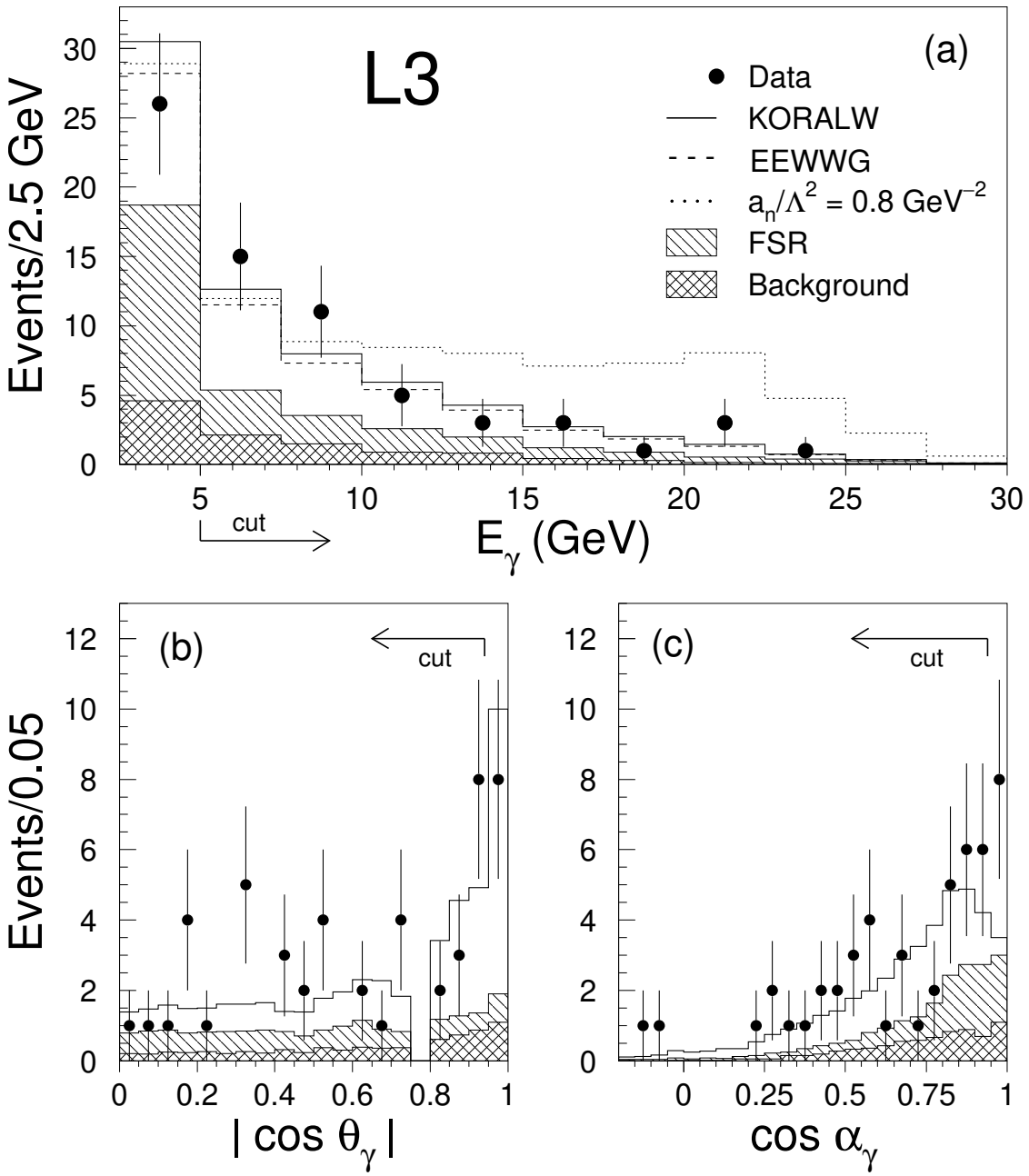

Figure 2: Differential distributions, for the semileptonic and fully hadronic $W^+W^-\gamma$ decay modes, of (a) the photon energy, (b) angle to the beam axis and (c) angle to the closest charged fermion respectively. The hatched area is the background component from ZZ, Zee, and $q\bar{q}(\gamma)$ events. Final state radiation includes the contribution of correctly identified photons radiated off the charged fermions and photons originating from isolated meson decays. In the upper plot, the distribution corresponding to a non-zero value of the anomalous coupling a_n/Λ^2 is shown as a dotted line.

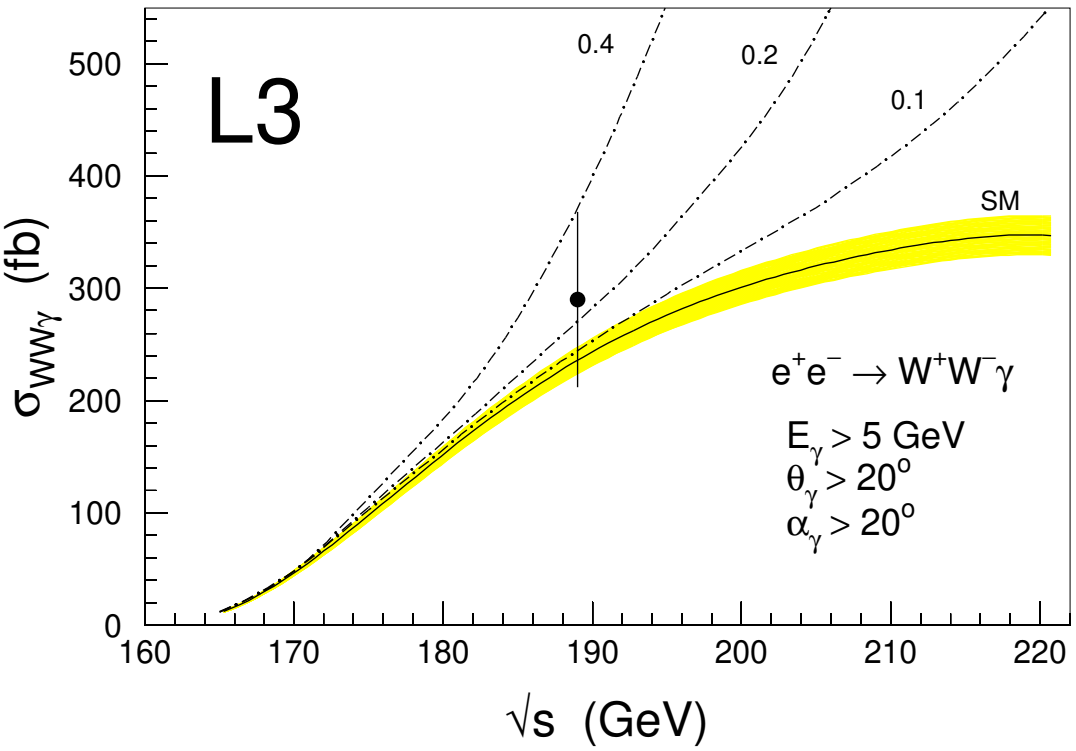

Figure 3: Standard Model (solid line) cross section for the process $e^+e^- \to W^+W^-\gamma$ as measured at $\sqrt{s} = 189$ GeV and as predicted by the EEWWG Monte Carlo within the indicated phase-space cuts. The shaded band corresponds to the theoretical uncertainty of $\pm 5\%$. The three dashed lines correspond to the cross section for non-vanishing values of the anomalous coupling a_n/Λ^2 (in GeV^{-2} units), as a function of the centre-of-mass energy.

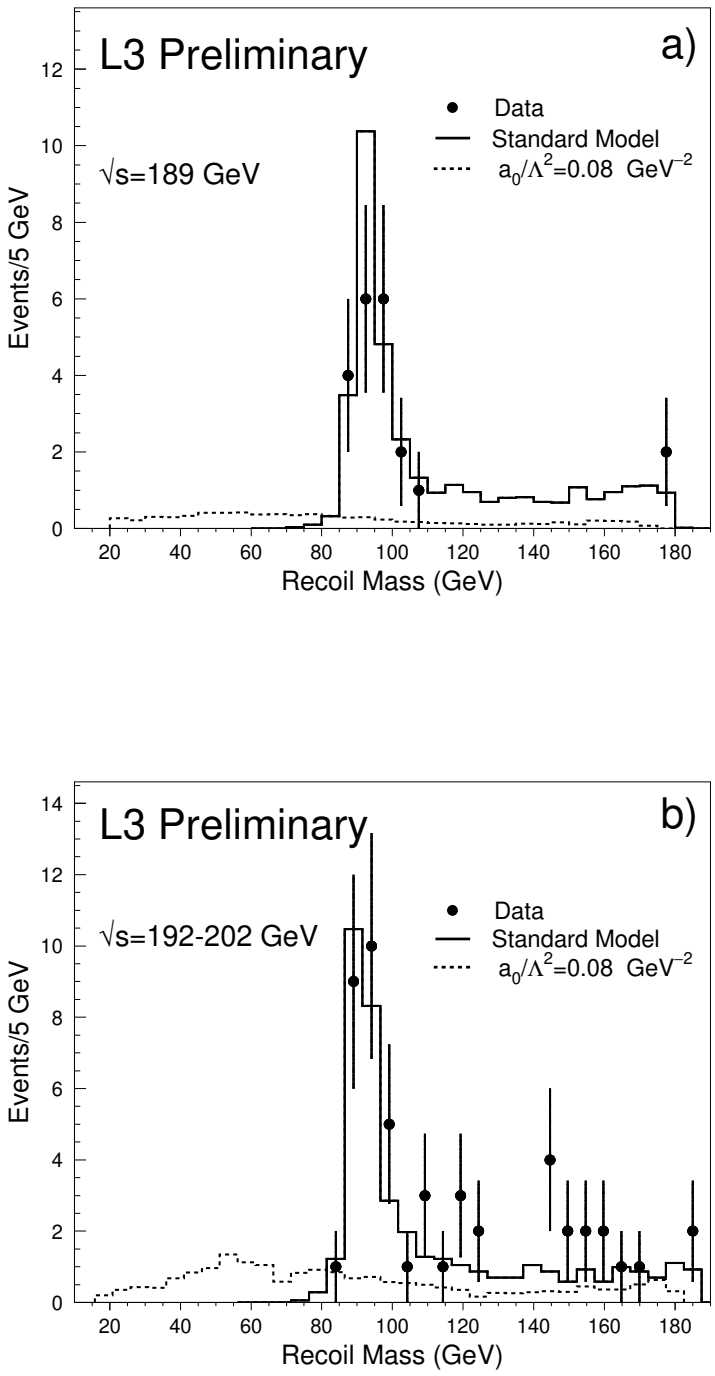

Figure 4: Recoil mass spectrum of the acoplanar photon pair events selected at (a) $\sqrt{s} = 189$ GeV and (b) $\sqrt{s} = 192 - 202$ GeV. Note that the AQGC signal prediction is reliable only for recoil masses lower than the mass of the Z boson (see explanation in the text).

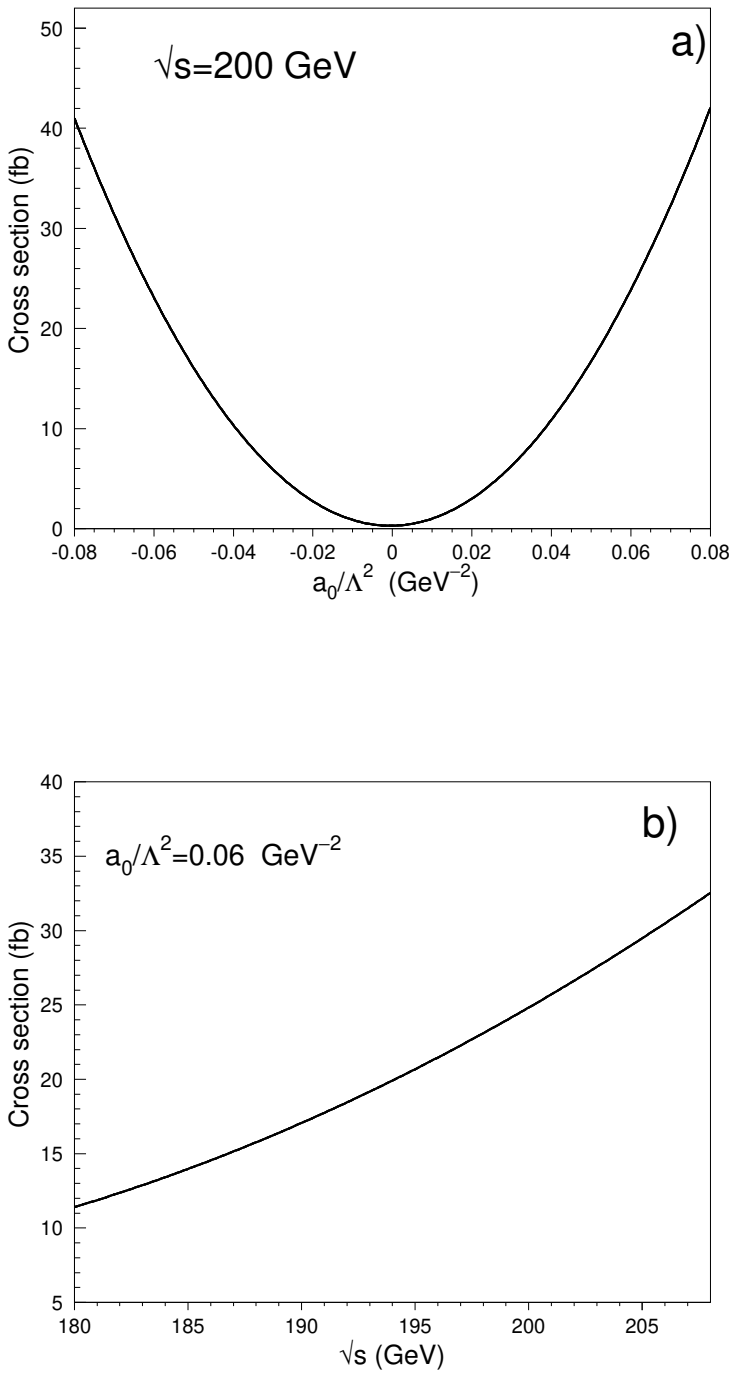

Figure 5: Cross section for the AQGC $\nu\bar{\nu}\gamma\gamma$ signal in the region $M_{rec} < M_{\rm Z}$ as a function of (a) the anomalous coupling a_0/Λ^2 and (b) the centre-of-mass energy.